0.5 µg pSV7neo, a plasmid conferring neomycin/G418 resistance, and 24 µg pBC12/PLseap plasmid as carrier DNA (ref. 18).

Molecular modeling. By using the coordinates of the wild-type p53 DNA binding domain bound to DNA (ref. 5), an Arg side chain was introduced at position 284 such that it would form electrostatic interactions with the phosphate oxygen atoms closest to its α-carbon and without violating bond lengths and angles. Modeling was performed with Quanta 4.1 (Molecular Simulations Inc., Burlington, Massachusetts), and the protein/DNA structures were drawn using Molscript (Per Kraulis) and Raster3D (David Bacon and Ethan Merritt).

Acknowledgments

We thank Guenther Karmann, Jim Elting, Giovanni Rovera, Jules Shafer, Frank Rauscher III, Ronen Marmorstein, Stanley Opella, Stephen Burley and Elena Stavridi for support and discussions. Also Nicola Pavletich for providing the coordinates of the p53-DNA complex and David Livingston for providing the Saos-2 cells. Financial support was provided by Bayer A.G.

RECEIVED 14 JUNE; ACCEPTED 5 AUGUST 1996

1. Kastan, M.B., Onyekwere, O., Sidransky, D., Vogelstein, B. & Craig, R.W. Participation of p53 protein in the cellular response to DNA damage. *Cancer Res.* **51**, 6304–6311 (1991).
2. Lowe, S.W. *et al. p53* status and the efficacy of cancer therapy in vivo. *Science* **266**, 807–810 (1994).
3. Ko, L.J. & Prives, C. p53: Puzzle and paradigm. *Genes Dev.* **10**, 1054–1072 (1996).
4. Hollstein, M., Sidransky, D., Vogelstein, B. & Harris, C.C. p53 mutations in human cancers. *Science* **253**, 49–53 (1991).
5. Cho, Y., Gorina, S., Jeffrey, P.D. & Pavletich, N.P. Crystal structure of a p53 tumor suppressor-DNA complex: Understanding tumorigenic mutations. *Science* **265**, 346–355 (1994).
6. Friend, S. p53: A glimpse at the puppet behind the shadow play. *Science* **265**, 334–335 (1994).
7. Halazonetis, T.D., Davis L.J. & Kandil, A.N. Wild-type p53 adopts a "mutant"-like conformation when bound to DNA. *EMBO J.* **12**, 1021–1028 (1993).
8. Hupp, T.R., Meek, D.W., Midgley, C.A. & Lane, D.P. Regulation of the specific DNA binding function of p53. *Cell* **71**, 875–886 (1992).
9. Waterman, J.L.F., Shenk, J.L. & Halazonetis, T.D. The dihedral symmetry of the p53 tetramerization domain mandates a conformational switch upon DNA binding. *EMBO J.* **14**, 512–519 (1995).
10. Halazonetis, T.D. & Kandil, A.N. Conformational shifts propagate from the oligomerization domain of p53 to its tetrameric DNA binding domain and restore DNA binding to select p53 mutants. *EMBO J.* **12**, 5057–5064 (1993).
11. Hupp, T.R., Meek, D.W., Midgley, C.A. & Lane, D.P. Activation of the cryptic DNA binding function of mutant forms of p53. *Nucleic Acids Res.* **21**, 3167–3174 (1993).
12. Niewolik, D., Vojtesek, B. & Kovarik, J. p53 derived from human tumour cell lines and containing distinct point mutations can be activated to bind its consensus target sequence. *Oncogene* **10**, 881–890 (1995).
13. Finlay, C.A. *et al.* Activating mutations for transformation by p53 produce a gene product that forms an hsc70-p53 complex with an altered half-life. *Mol. Cell. Biol.* **8**, 531–539 (1988).
14. El-Deiry, W.S. *et al. WAF1*, a potential mediator of p53 tumor suppression. *Cell* **75**, 817–825 (1993).
15. Kastan, M.B. *et al.* A mammalian cell cycle checkpoint pathway utilizing p53 and *GADD45* is defective in ataxia-telangiectasia. *Cell* **71**, 587–597 (1992).
16. Kern, S.E. *et al.* Oncogenic forms of p53 inhibit p53-regulated gene expression. *Science* **256**, 827–830 (1992).
17. Finlay, C.A., Hinds, P.W. & Levine, A.J. The p53 proto-oncogene can act as a suppressor of transformation. *Cell* **57**, 1083–1093 (1989).
18. Waterman, M.J.F., Waterman, J.L.F. & Halazonetis, T.D. An engineered four-stranded coiled coil substitutes for the tetramerization domain of wild-type p53 and alleviates transdominant inhibition by tumor-derived p53 mutants. *Cancer Res.* **56**, 158–163 (1996).
19. Symonds, H. *et al.* p53-dependent apoptosis suppresses tumor growth and progression in vivo. *Cell* **78**, 703–711 (1994).
20. Graeber, T.G. *et al.* Hypoxia-mediated selection of cells with diminished apoptotic potential in solid tumours. *Nature* **379**, 88–91 (1996).

The E280A presenilin 1 Alzheimer mutation produces increased Aβ42 deposition and severe cerebellar pathology

CYNTHIA A. LEMERE[1], FRANCISCO LOPERA[2], KENNETH S. KOSIK[1], CORRINE L. LENDON[3], JORGE OSSA[2], TAKAOMI C. SAIDO[4], HARUYASU YAMAGUCHI[5], ANDRES RUIZ[2], ALONSO MARTINEZ[2], LUCIA MADRIGAL[2], LILIANA HINCAPIE[2], JUAN CARLOS ARANGO L.[2], DOUGLAS C. ANTHONY[6], EDWARD H. KOO[1,6], ALISON M. GOATE[3], DENNIS J. SELKOE[1] & JUAN CARLOS ARANGO V.[2]

[1]Center For Neurologic Diseases and [6]Department of Pathology, Harvard Medical School, Brigham and Women's Hospital, LMRC 103b, 221 Longwood Avenue, Boston, Massachusetts 02115 USA
[2]Departments of Neurology, Biochemistry and Pathology, Universidad de Antioquia, Medellín, Colombia
[3]Departments of Psychiatry and Genetics, Washington University School of Medicine, St. Louis, Missouri 63110 USA
[4]Department of Molecular Biology, Tokyo Metropolitan Institute of Medical Science, Tokyo, Japan
[5]College of Medical Care and Technology, Gunma University, Gunma, Japan
Correspondence should be addressed to D.J.S.
e-mail: selkoe@cnd.bwh.harvard.edu

Missense mutations in the presenilin 1 (*PS1*) gene cause the most common form of dominant early-onset familial Alzheimer's disease (FAD)[1,2] and are associated with increased levels of amyloid β-peptides (Aβ) ending at residue 42 (Aβ42) in plasma and skin fibroblast media of gene carriers[3]. Aβ42 aggregates readily and appears to provide a nidus for the subsequent aggregation of Aβ40 (ref. 4), resulting in the formation of innumerable neuritic plaques. To obtain *in vivo* information about how *PS1* mutations cause AD pathology at such early ages, we characterized the neuropathological phenotype of four PS1-FAD patients from a large Colombian kindred[5] bearing the codon 280 Glu to Ala substitution (Glu280Ala) PS1 mutation[2]. Using antibodies specific to the alternative carboxy-termini of Aβ, we detected massive deposition of Aβ42, the earliest and predominant form of plaque Aβ to occur in AD (ref. 6–8), in many brain regions. Computer-assisted quantification revealed a significant increase in Aβ42, but not Aβ40, burden in the brains from 4 PS1-FAD patients compared with those from 12 sporadic AD patients. Severe cerebellar pathology included numerous Aβ42-reactive plaques, many bearing dystrophic neurites and reactive glia. Our results in brain tissue are consistent with recent biochemical evidence of increased Aβ42 levels in PS1-FAD patients and strongly suggest that mutant PS1 proteins alter the proteolytic processing of the β-amyloid precursor protein at the C-terminus of Aβ to favor deposition of Aβ42.

To examine C-terminal Aβ immunoreactivity in the four PS1-FAD brains, we stained adjacent tissue sections with polyclonal antibodies specific for Aβ peptides ending at residues 40, 42 or

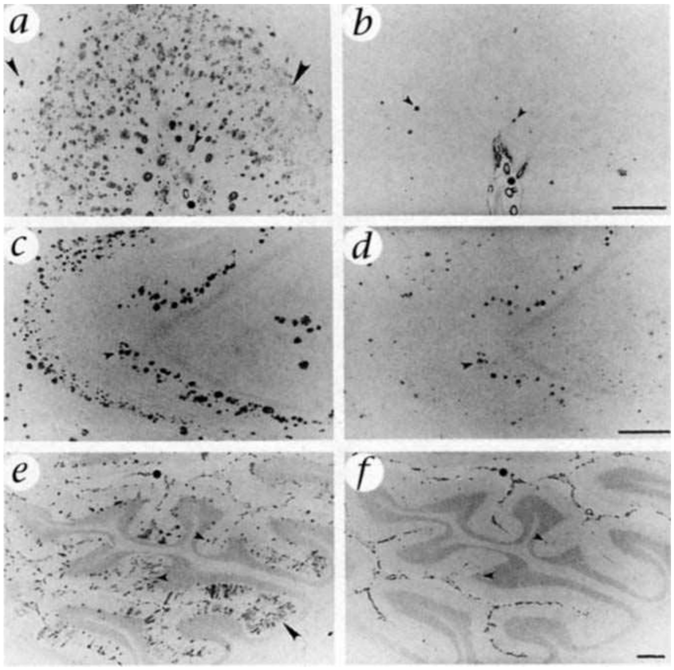

Fig. 1 Aβ42 is detected in much greater quantity than Aβ40 in PS1-FAD brains. *a*, Large numbers of Aβ42-IR plaques are present in frontal cortex, including compacted plaques in all layers (small and medium arrowheads) and a diffuse Aβ42 band in layer IV (large arrowhead). *b*, A few compacted Aβ40-IR plaques (small arrowheads) and blood vessels occur in an adjacent section to that shown in *a*. Note that most of the Aβ40-positive blood vessels are also Aβ42-IR (asterisk). *c*, Many intensely Aβ42-IR plaques (arrowhead) are present just outside the dentate gyrus and in CA1 and subiculum in the hippocampus. *d*, A subset of Aβ42-containing plaques are also Aβ40-IR (for example, arrowheads in *d* and *c*) in a section adjacent to that shown in *c*. *e*, Numerous Aβ42-IR plaques occur in cerebellum, including diffuse plaques in the molecular layer (large arrowhead) and compacted plaques in the molecular, Purkinje cell and granule cell layers (small arrowheads). Many leptomeningeal blood vessels are also Aβ42-IR (asterisk). *f*, A minority of compacted plaques in the Purkinje cell layer (left arrowhead) and molecular layer (right arrowhead) and leptomeningeal blood vessels (for example, asterisk) are labeled by Aβ40 antibody in an adjacent section to that shown in *e*. *a–d*, A 47-year-old patient with *PSl* mutation; *e* and *f*, A 62-year-old patient with *PSl* mutation. Scale bars, 500 μm.

43 (ref. 9, 10). Massive numbers of Aβ42-immunoreactive (IR) plaques were detected in cerebral cortex, hippocampus and cerebellum (Fig. 1, *a*, *c* and *e*). Many Aβ42-IR diffuse plaques occurred in midbrain, caudate and other basal ganglia. Fewer plaques were immunoreactive for Aβ40 (Fig. 1, *b*, *d* and *f*) or Aβ43 (not shown); these were mostly compacted[8] plaques. In cerebellum, Aβ42-IR diffuse plaques occurred primarily in the molecular layer, whereas Aβ42-IR compacted plaques, some having discrete round cores, were detected in the molecular, Purkinje cell and granule cell layers (Fig. 1*e*). Some compacted plaques were Aβ40-IR (Fig. 1*f*) . Prominent amyloid angiopathy was detected in all four PS1-FAD brains, particularly in occipital cortex and cerebellum (Fig. 2, *a–c*). Aβ40 was dominant in blood vessels. Virtually all Aβ40-positive vessels contained substantial Aβ42-IR, in contrast to sporadic AD, in which only a small subset of vessels were Aβ42-IR. Fewer Aβ43-IR vessels were observed. Striking deposits of Aβ42-IR perivascular and subpial Aβ were seen (Fig. 2*d*).

Neuritic alterations and astrocytosis typical of AD were seen in cerebral cortex and hippocampus of all four PS1-FAD brains. Many neurofibrillary tangles and neuritic plaques were detected by tau and ubiquitin antibodies throughout cortex and hippocampus. Regions of heavy Aβ plaque deposition were infiltrated by numerous reactive astrocytic processes.

An unusually large number of Aβ42 plaques was observed in cerebellum in all four PS1-FAD patients (for example, Fig. 1*e*). Ubiquitin-positive dystrophic neurites often colocalized with compacted Aβ42-IR plaques in the molecular layer (Fig. 3, *a* and *b*) and to a lesser extent in the Purkinje cell layer. Cerebellums from 3 of the 12 sporadic AD patients showed some ubiquitin reactivity; however, the numbers of ubiquitin-positive plaques were much lower than those observed in the PS1-FAD cases. Only a small subset of the ubiquitin-reactive plaques in the cerebellums from patients with the PS1 mutation were Aβ40-positive (Fig. 3, *b* and *c*). Bielschowsky stain revealed dystrophic neurites in a small subset of ubiquitin-IR cerebellar plaques, particularly in the Purkinje cell layer, in the PS1-FAD cases. All cerebellar plaques were tau-negative. Unlike the situation in the 12 sporadic AD brains, glial fibrillary acidic protein (GFAP)-positive reactive astrocytes colocalized with numerous compacted Aβ42-immunoreactive plaques in cerebellum (Fig. 3, *d* and *e*); astrocytic processes appeared to infiltrate entire plaques. In addition, GFAP-positive astrocytes were detected in cerebellar white matter (Fig. 3*f*) in brains of patients with PS1-FAD but not sporadic AD. Previously, occasional cerebellar pathology was reported in some chromosome 14-linked families[11,12]. However, we found robust cerebellar pathology in all four patients with E280A PS1. The severity of the cerebellar changes in PS1-FAD brain cannot be attributed to disease duration, because these cases were symptomatic for a shorter time than most of the sporadic AD cases. High cerebellar PS1 mRNA expression[13] may be relevant to the striking cerebellar pathology.

To compare Aβ immunoreactivity in the brains from 4 PS1-FAD and 12 sporadic AD patients, we used computer-assisted image analysis to quantify the percentage of brain area containing maximal Aβ42 (C42) and maximal Aβ40 (BC40) immunoreactivity in adjacent sections from four brain regions for each case. For sampling consistency, the area in each section with the highest plaque density was selected for quantification. The greater Aβ42 reactivity in the four PS1-FAD brains was highly significant ($P \le 0.002$; two-tailed Mann-Whitney U-test) in all brain regions examined. Indeed, each brain region in all four PS1-FAD cases showed a higher percentage of area occupied by Aβ42 than did the corresponding region in all 12 sporadic AD cases, with just one exception (Aβ42 was slightly higher in the temporal cortex of 1 of the 12 sporadic AD than in 1 of the 4 PS1-FAD brains). This striking difference is highlighted by the complete separation of the standard deviations of the two patient groups (Fig. 4*a*). The percentage of area occupied by Aβ40 varied markedly among cases within each group. The three cortical areas examined showed no significant increase in Aβ40 burden in PS1-FAD; only the cerebellum had a significant ($P \le 0.001$) increase. Rank ordering the cortical Aβ40 values for all 16 cases confirmed that the PS1-FAD cases were not clustered at the top of the rank, but randomly distributed, as expected from the

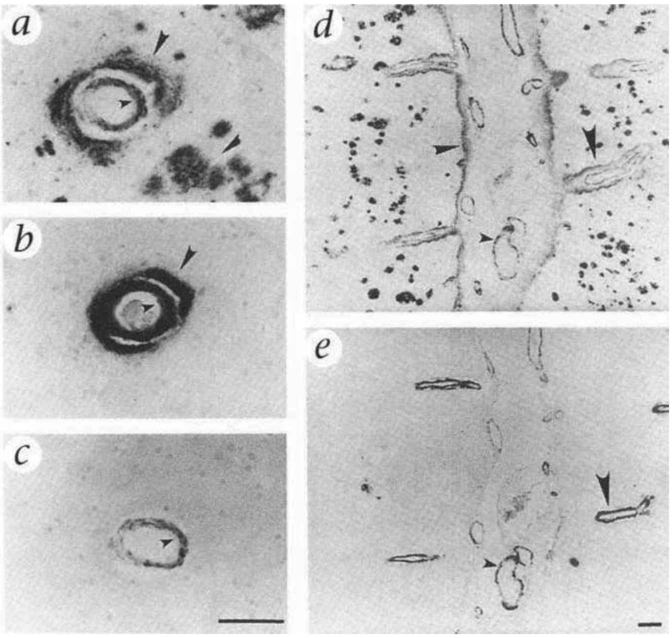

Fig. 2 Many Aβ42-IR blood vessels, in addition to more typical Aβ40-IR blood vessels, are observed in PS1-FAD brains. *a*, Aβ42 is present in the wall of a frontal cortex arteriole in the 47-year-old patient (small arrowhead). Note extensive perivascular and plaque immunoreactivity surrounding the vessel (large arrowheads). *b*, The blood vessel wall (small arrowhead) and perivascular deposit (large arrowhead) are Aβ40-IR in a section adjacent to that shown in *a*. *c*, The wall of the blood vessel in *a* and *b* is also reactive for Aβ43, but perivascular and plaque reactivity are absent. *d*, In addition to plaques, numerous leptomeningeal (small arrowhead) and parenchymal (large arrowhead) blood vessels are Aβ42-IR in occipital cortex of the 62-year-old patient. Note intense perivascular immunoreactivity surrounding the parenchymal blood vessels (large arrowhead). Subpial Aβ42 deposits (medium arrowheads) are often continuous with perivascular staining close to the pial surface. *e*, The same blood vessels are Aβ40-IR in a section adjacent to that shown in *d* (arrowheads). Very few plaques and no perivascular deposits are Aβ40-IR. Scale bars, 100 μm.

complete overlap of the large standard deviations (Fig. 4*b*). Next, semiquantitative scoring (0–4+) of the Aβ40 burden over the entire section was conducted independently by two of us (C.A.L. and D.J.S.) and again showed both the large variation in amount of Aβ40 within each patient group and the lack of difference between the groups. This semiquantitative result was confirmed using a monoclonal antibody [BA27 (ref. 6)] specific for Aβ40, which produced staining similar to that of BC40.

Here, we demonstrate a distinct neuropathological phenotype for the PS1-FAD genotype in four patients all bearing the same presenilin mutation (E280A) expressed within a relatively homogeneous genetic background. In addition to conventional AD features (abundant senile plaques and neurofibrillary tangles), the brains of all four PS1-FAD patients showed massive Aβ42 deposition, prominent gliosis and severe cerebellar pathology; these changes occurred ~30 years earlier than those in the 12 sporadic AD patients. An increase in cerebral and cerebrovascular Aβ burden in late-onset AD subjects harboring one or two apolipoprotein E (apoE) ε4 alleles has been demonstrated[14,15]. The Aβ42 increase in our PS1-FAD subjects cannot be explained by an apoE effect, because only one patient carried an ε4 allele, and the 12 sporadic cases (selected for severe AD neuropathology) showed the expected overrepresentation of ε4 alleles relative to the general population.

Our findings of increased Aβ42 deposition in PS1-FAD brain parenchyma and blood vessels support recent biochemical evidence of significantly increased Aβ42 levels in plasma and skin fibroblast media from numerous PS1-FAD patients[3,16]. The importance of Aβ42 deposition in AD pathogenesis has been suggested by these observations: Aβ42 is the earliest Aβ species deposited in the brain[6–9]; it readily forms fibrillar amyloid aggregates *in vitro*; and it can act as a nidus for Aβ40 deposition[4,17].

Increased levels of Aβ42 have also been observed in FAD caused by amyloid β-protein precursor (βAPP) mutations. Missense mutations at βAPP codon 717 result in increased amounts of Aβ42 in brain, as detected both biochemically[18] and

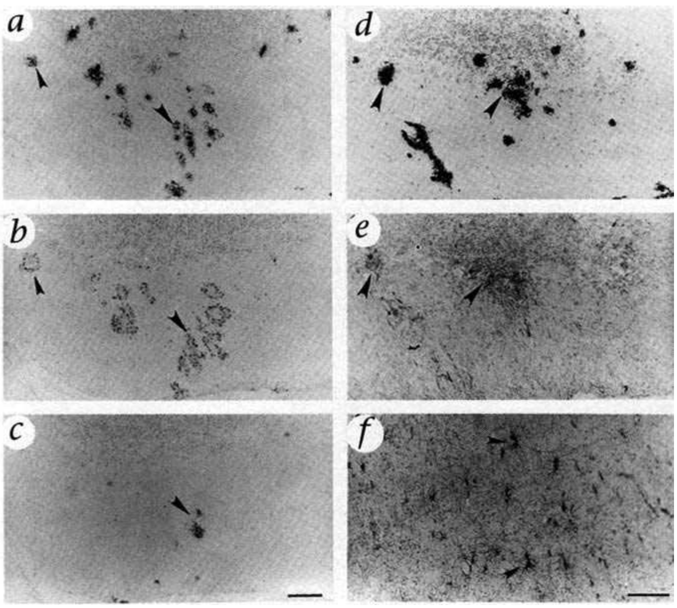

Fig. 3 Severe cerebellar pathology occurs in the PS1-FAD patients. *a*, Abundant Aβ42-IR plaques are seen in the molecular (for example, arrowheads) and Purkinje cell layers in the 62-year-old patient. *b*, In an adjacent section, many ubiquitin-IR dystrophic neurites occur in the periphery of plaques that colocalize with those in *a* (for example, arrowheads). *c*, A very small number of Aβ40 plaques (arrowhead) are present in molecular layer in an adjacent section. *d*, In another region of cerebellum, Aβ42 plaques occur in the molecular (for example, left arrowhead) and Purkinje cell (for example, right arrowhead) layers. *e*, In an adjacent section, reactive astrocytes detected by anti-GFAP colocalize with some plaques (arrowheads) shown in *d*. *f*, Many GFAP-IR astrocytes are found in cerebellar white matter. Scale bars, 100 μm.

immunocytochemically[6,19]. Furthermore, cells expressing βAPP717 mutant cDNAs secrete increased levels of Aβ42 (ref. 20). The "Swedish" double mutation at βAPP670/671 increases both Aβ40 and Aβ42 in brain deposits[19], in cells transfected with this isoform[21,22], and in primary skin fibroblasts[23] and plasma[3]. Our findings are entirely consistent with the hypothesis that the βAPP- and presenilin-linked forms of FAD are initiated by overproduction of highly aggregable Aβ42 peptides. Such overproduction would then lead to increased tissue deposition, gradual compaction of plaques and, ultimately, the neuritic and glial cytopathology observed around mature plaques in AD.

Taken together, our data and those of Scheuner *et al.*[3] indicate that *PS1* missense mutations lead to altered proteolytic processing of βAPP at the C-terminus of Aβ, resulting in increased production and deposition of Aβ42 in plaques and blood vessels. Because elevated Aβ42 levels have already been documented in subjects bearing several different *PS1* or *PS2* mutations[3], we hypothesize that the very high Aβ42 burden seen here will be found in other presenilin kindreds. In another study, Mann *et al.*[24] found an increase in both Aβ42- and Aβ40-burden in some PS1-FAD cases, although other patients in their study had Aβ40 burdens similar to those in sporadic AD. Thus, it appears that the mechanistic effect of *PS1* mutations leading to severe, early-onset AD consistently involves an early increase in Aβ42 production and deposition and does not necessarily require a concomitant increase in Aβ40 production. It follows that, in some cases, the overwhelming burden of Aβ42 may lead to further deposition of Aβ40, the level of which could be determined in part by apoE genotype, duration of the disease or other factors. Alternatively, increased Aβ40 burden may be mutation specific. Because Aβ42 is the initially deposited species in AD, Down syndrome and aged human brains, our findings have implications for all forms of AD.

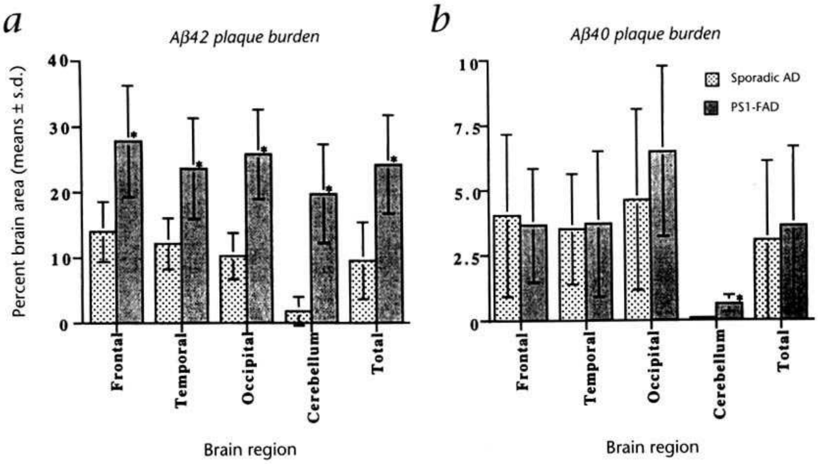

Fig. 4 Computer-assisted quantitative image analysis of Aβ42 and Aβ40 burdens in the regions of densest plaque immunoreactivity per antibody (adjacent sections) in brains from 4 PS1-FAD and the 12 sporadic AD patients. *a*, Means (± s.d.) of the percentages of brain area of maximal Aβ42-reactivity (quantified over an area of 3.72 mm^2) in indicated brain regions in brains from 4 PS1-FAD and 12 sporadic AD patients. Aβ42 levels were significantly higher (*) in PS1-FAD than sporadic AD cases for all regions tested. Two-tailed *P* values (Mann-Whitney U-test for nonparametric statistical analysis) were: frontal, $P = 0.0011$; temporal, $P = 0.0022$; occipital, $P = 0.0011$; cerebellum, $P = 0.0011$; average of all 4 regions, $P < 0.0001$. *b*, Means (± s.d.) of the percentages of brain area of maximal Aβ40-reactivity (quantified over an area of 3.72 mm^2) in indicated brain regions for all 4 PS1-FAD and 12 sporadic AD patients. Aβ40 levels were not significantly higher in PS1-FAD than sporadic AD cases in all three cortical areas tested. Note the large, overlapping standard deviations observed with Aβ40. A significant increase in Aβ40 ($P = 0.001$) was found in PS1-FAD cerebellum.

Methods

Subjects. Four autopsy brains [patients aged 47–62 years (mean, 54 years); mean duration of illness, 7.5 years] from a Colombian FAD kindred with the E280A missense mutation in the presenilin 1 (*PS1*) gene[2] were examined by immunocytochemical and histological methods. The E280A *PS1* genotype was confirmed for three of these patients (by C.L.L.). A lack of frozen tissue or blood sample prevented genotyping of the fourth patient from this kindred (no. 209 in Table 1). However, an affected sibling and adult child of this patient both bear the E280A *PS1* mutation. The spouse of the patient remains unaffected at age 61. For quantitative comparison of Aβ42 burden, autopsy brains from 12 sporadic AD subjects [ages 75–94 years (mean, 84 years); mean duration of illness, 10.5 years)] with moderate or severe AD neuropathology were also examined. ApoE genotype analysis was performed (by C.L.L.) on 3 of 4 PS1-FAD and 10 of 12 sporadic AD cases (see Table 1).

Immunocytochemistry. Blocks of brain tissue were routinely fixed in 10% neutral buffered formalin for 2 weeks to 2 months. After paraffin embedding of the blocks, 8-μm serial sections were cut and baked at 58 °C for 1 h. Three cortical areas (frontal, temporal and occipital) and cerebellum were examined in all 4 FAD and 12 sporadic AD cases. In addition, hippocampus, caudate, other basal ganglia and midbrain from the four FAD cases were examined.

Brain sections from FAD cases were stained immunocytochemically by the avidin-biotin horseradish peroxidase/DAB method (rabbit or mouse ABC Elite kit, Vector Laboratories, Burlingame, California) with the following primary antibodies: end-specific C-terminal Aβ polyclonal antibodies C42, C40 and C43 (1:250)[10] and BC42 and BC40 (1:500)[9] for detection of Aβ ending at residues 40, 42 or 43; and a polyclonal antibody against GFAP (1:1000) (gift of D. Dahl) for detection of reactive astrocytes. For detection of neurofibrillary tangles and dystrophic neurites, two antibodies were used: a polyclonal antibody against ubiquitin (1:2000) (East Acres Antibodies, Boston, Massachusetts) and a monoclonal antibody, 5E2 (ref. 25), against tau protein (1:500). Sections from the 12 sporadic AD brains were also immunostained with the end-specific C-terminal Aβ, GFAP and ubiquitin antibodies listed above. Formic acid pretreatment (88% for 20 minutes at room temperature) was used with the C-terminal Aβ and ubiquitin antibodies to enhance immunoreactivity. Microwave pretreatment (antigen retrieval protocol, BioGenex, San Ramon, California) was used with antibody 5E2. Specificity of all other antibodies has been previously demonstrated (see antibody references cited above). All sections were incubated with primary antibodies overnight at 4 °C. Omission of primary antibody consistently yielded negative results. FAD brain sections were also stained by a modified Bielschowsky silver method.

Quantification. Access to a Quantimet image analyzer was kindly provided by E. Masliah (Univ. California–San Diego School of Medicine, San Diego, California). A background threshold intensity was determined in an area of each stained section devoid of immunoreactivity. Detection of immunoreactivity above that threshold was then measured. Aβ burdens were quantified in four brain regions: frontal, temporal and occipital cortices and cerebellum. The percentage of brain area of maximal Aβ42 (antibody C42) and maximal Aβ40 (antibody BC40) immunoreactivity was determined for six ×10 microscopic fields (total area: 3.72 mm²). By using two immediately adjacent sections stained with anti-Aβ42 or anti-Aβ40, the regions of highest plaque density in each section were visually selected for the computerized quantification in each of the 4 FAD and 12 sporadic AD cases. Immunoreactive blood vessels were edited out before quantification. A nonparametric statistical test, the Mann-Whitney U-test, was performed to compare the percentages of brain area occupied by Aβ42- and Aβ40-immunoreactive plaques in the 4 FAD versus 12 sporadic AD cases in each of the four brain regions. In addition, semiquantitative visual assessments (scoring 0–4+) for each Aβ40-stained section were made independently by two investigators (C.A.L. and D.J.S.).

Table 1 Case descriptions

Case no.	Diagnosis	Sex	Age of onset (yr)	Duration of illness (yr)	Age at death (yr)	ApoE genotype
209	PS1-FAD	F	48	9	57	NA
210	PS1-FAD	M	54	8	62	3/3
211	PS1-FAD	M	45	5	50	3/3
212	PS1-FAD	F	39	8	47	3/4
			mean 46.5	mean 7.5	mean 54	
1745	AD	F	73	7	80	3/3
2038	AD	M	70	7	77	3/4
2044	AD	F	71	13	84	4/4
2045	AD	M	79	8	87	NA
2069	AD	F	72	10	82	3/4
2108	AD	F	68	20	88	3/3
93-103	AD	M	70	6	76	NA
94-19	AD	F	80	10	90	3/3
94-197	AD	F	74	15	89	2/3
94-239	AD	F	71	14	85	4/4
94-270	AD	F	84	10	94	3/4
95-6	AD	M	69	6	75	3/4
			mean 73.4	mean 10.5	mean 83.9	

NA, not available.

Acknowledgments

We thank Eliezer Masliah and Richard DeTeresa for providing use of the Quantimet image analyzer and Ronald Bosch and Adriana Ferreira for helpful discussions. This work was supported by National Institutes of Health grant AG 06173 and the Foundation for Neurologic Diseases (to D.J.S.), by Colciencias projecto 1115-04-040-95 at Univ. de Antioquia (to F.L.), and by National Institute on Aging career development award AG 00634 (to A.M.G.).

RECEIVED 28 JUNE; ACCEPTED 20 AUGUST 1996

1. Sherrington, R. *et al.* Cloning of a novel gene bearing missense mutations in early onset familial Alzheimer disease. *Nature* **375**, 754–760 (1995).
2. Clark, R.F. *et al.* The structure of the presenilin 1 (S182) gene and identification of six novel mutations in early onset AD families. *Nature Genet.* **11**, 219–222 (1995).
3. Scheuner, D. *et al.* Secreted amyloid β-protein similar to that in the senile plaques of Alzheimer's disease is increased *in vivo* by the presenilin 1 and 2 and *APP* mutations linked to familial Alzheimer's disease. *Nature Med.* **2**, 864–870 (1996).
4. Jarrett, J.T. & Lansbury, P.T., Jr. Seeding "one-dimensional crystallization" of amyloid: A pathogenic mechanism in Alzheimer's disease and scrapie? *Cell* **73**, 1055–1058 (1993).
5. Lopera, F. *et al.* Demencia tipo Alzheimer con agregación familiar en Antioquia, Colombia. *Acta Neurol. Colombiana* **10**, 173–187 (1994).
6. Iwatsubo, T. *et al.* Visualization of A beta 42(43) and A beta 40 in senile plaques with end-specific A beta monoclonals: Evidence that an initially deposited species is A beta 42(43). *Neuron* **13**, 45–53 (1994).
7. Iwatsubo, T., Mann, D.M., Odaka, A., Suzuki, N. & Ihara, Y. Amyloid β protein (Aβ) deposition: Aβ42(43) precedes Aβ40 in Down syndrome. *Ann. Neurol.* **37**, 294–299 (1995).
8. Lemere, C.A. *et al.* Sequence of deposition of heterogeneous amyloid β-peptides and Apo E in Down syndrome: Implications for initial events in amyloid plaque formation. *Neurobiol. Dis.* **3**, 16–32 (1996).
9. Yamaguchi, H., Sugihara, S., Ishiguro, K., Takashima, A. & Hirai, S. Immunohistochemical analysis of COOH-termini of amyloid beta protein (Aβ) using end-specific antisera for Aβ40 and Aβ42 in Alzheimer's disease and normal aging. *Amyloid Int. J. Clin. Invest.* **2**, 7–16 (1995).
10. Saido, T.C. *et al.* Dominant and differential deposition of distinct β-amyloid peptide species, $A\beta_{N3(p3)}$, in senile plaques. *Neuron* **14**, 457–466 (1995).
11. Haltia, M. *et al.* Chromosome 14-encoded Alzheimer's disease: Genetic and clinicopathological description. *Ann. Neurol.* **36**, 362–367 (1994).
12. Lampe, T.H. *et al.* Phenotype of chromosome 14-linked familial Alzheimer's disease in a large kindred. *Ann. Neurol.* **36**, 368–378 (1994).
13. Kovacs, D.M. *et al.* Alzheimer-associated presenilins 1 and 2: Neuronal expression in brain and localization to intracellular membranes in mammalian cells. *Nature Med.* **2**, 224–229 (1996).
14. Schmechel, D.E. *et al.* Increased amyloid β-peptide deposition in cerebral cortex as a consequence of apolipoprotein E genotype in late-onset Alzheimer disease. *Proc. Natl. Acad. Sci. USA* **90**, 9649–9653 (1993).
15. Greenberg, S.M., Rebeck, G.W., Vonsattel, J.P.G., Gomez-Isla, T. & Hyman, B.T. Apolipoprotein E ε4 and cerebral hemorrhage associated with amyloid angiopathy. *Ann. Neurol.* **38**, 254–259 (1995).
16. Song, X.-H. *et al.* Plasma amyloid β protein (Aβ) is increased in carriers of familial AD (FAD) linked to chromosome 14. *Soc. Neurosci. Abstr.* **21**, 1501 (1995).
17. Jarrett, J.T., Berger, E.P. & Lansbury, P.T., Jr. The carboxy terminus of the beta amyloid protein is critical for the seeding of amyloid formation: Implications for the pathogenesis of Alzheimer's disease. *Biochemistry* **32**, 4693–4697 (1993).
18. Tamaoka, A. *et al.* APP717 missense mutation affects the ratio of amyloid β protein species (Aβ1–42/43 and Aβ1–40) in familial Alzheimer's disease brain. *J. Biol. Chem.* **269**, 32721–32724 (1994).
19. Mann, D.M.A. *et al.* Predominant deposition of amyloid-$\beta_{42(43)}$ in plaques in cases of Alzheimer's disease and hereditary cerebral hemorrhage associated with mutations in the amyloid precursor protein gene. *Am. J. Pathol.* **148**, 1257–1266 (1996).
20. Suzuki, N. *et al.* An increased percentage of long amyloid β protein secreted by familial amyloid β protein precursor (βAPP717) mutants. *Science* **264**, 1336–1340 (1994).
21. Citron, M. *et al.* Mutation of the β-amyloid precursor protein in familial Alzheimer's disease increases β-protein production. *Nature* **360**, 672–674 (1992).
22. Cai, X.-D., Golde, T.E. & Younkin, G.S. Release of excess amyloid β protein from a mutant amyloid β protein precursor. *Science* **259**, 514–516 (1993).
23. Citron, M. *et al.* Excessive production of amyloid β-protein by peripheral cells of symptomatic and presymptomatic patients carrying the Swedish familial Alzheimer's disease mutation. *Proc. Natl. Acad. Sci. USA* **91**, 11993–11997 (1994).
24. Mann, D.M.A. *et al.* Amyloid β protein (Aβ) deposition in chromosome 14-linked Alzheimer's disease: Predominance of Aβ42(43). *Ann. Neurol.* **40**, 149–156 (1996).
25. Kosik, K.S. *et al.* Epitopes that span the tau molecule are shared with paired helical filaments. *Neuron* **1**, 817–825 (1988).